

Investigating the Structure and Properties of Hydrated Hydroxypropyl Methylcellulose and Egg Albumin Matrices Containing Carbamazepine: EPR and NMR Study

Ifat Katzhendler,¹ Karsten Mäder,² Reuven Azoury,³ and Michael Friedman^{1,4,5}

Received March 18, 2000; accepted June 22, 2000

Purpose. The present study was conducted in order to investigate the correlation between the hydration properties of HPMC and EA matrices, gel microstructure and mobility, crystalline changes occurring in the gel and CBZ release kinetics. The influence of HPMC and EA erosion modes on CBZ release kinetics was interpreted in terms of gel microstructures.

Methods. NMR technique was used to determine the T_1 and T_2 relaxation rates of water in hydrated matrices. PFGSE NMR technique was employed to determine the SDC of water in the gels. EPR technique was used to determine the rotational correlation time of PCA in the hydrated matrices, gel microviscosity, mobile compartment, α , β , γ parameters and lorentzian/gaussian ratio. These parameters are indicative of matrix microstructure.

Results. CBZ release mechanism from HPMC and EA matrices was markedly different. This behavior was related to the different structures of the polymer and protein. T_2 relaxation studies and SDC measurements by NMR revealed higher chain hydration for HPMC compared to EA. Using the EPR technique it has been shown that the microviscosity and mobile compartment of matrices containing HPMC are lower than matrices containing EA. The microviscosity, mobile compartment and S -parameter values of hydrated matrices containing different EA/CBZ ratios were in correlation with the crystallization properties of CBZ in the gels, matrix erosion properties and CBZ release kinetics from the matrices.

Conclusions. Characterization of matrix structures using EPR and NMR techniques supported our hypothesis concerning the mechanism involved in HPMC-CBZ interaction. EA/CBZ matrix microstructure features, analyzed by NMR and EPR techniques, were in correlation with the crystalline changes occurring in the gel and drug release kinetics.

KEY WORDS: carbamazepine; hydroxypropylmethylcellulose; egg albumin; electron paramagnetic resonance; nuclear magnetic resonance.

¹ Department of Pharmaceutics, School of Pharmacy, The Hebrew University of Jerusalem, P.O.B. 12065, Jerusalem 91120, Israel.

² Department of Pharmaceutics, Free University, Kelchstr. 31, 12169 Berlin, Germany.

³ Radiopharmaceutical Division, Soreq N.R.C., 10800 Yavne, Israel.

⁴ Affiliated with the David R. Bloom Center for Pharmacy at the Hebrew University of Jerusalem.

⁵ To whom correspondence should be addressed. (e-mail: mikef@cc.huji.ac.il)

ABBREVIATIONS: CBZ, carbamazepine; EA, egg albumin; EPR, electron paramagnetic resonance; HPMC, hydroxypropyl methylcellulose; NMR, nuclear magnetic resonance; PFGSE, pulse field gradient spin echo; PCA, 3-carboxy proxyl; SDC, self diffusion coefficient.

INTRODUCTION

In our previous research (1,2) we investigated the influence of hydroxypropyl methylcellulose (HPMC) and egg albumin (EA) on the crystalline properties and polymorphic transitions of carbamazepine (CBZ) using Differential Scanning Calorimeter (DSC), Hot-Stage Microscopy (HSM), X-ray powder diffraction (XRD), Scanning Electron Microscopy (SEM) and Contact Angle Goniometer (CAG). The results suggested that HPMC and EA affected the crystalline properties and polymorphic transitions of CBZ in the solid state, aqueous solutions and in the gel layer of hydrated tablets. In aqueous solutions containing HPMC and EA, the polymer (and protein) inhibited the transformation of CBZ to CBZ dihydrate form. This effect depended on HPMC and EA concentrations. The inhibition of CBZ transformation to its dihydrate form was more effective with HPMC and occurred at molar concentrations of 100 times less in comparison to EA. In the gel layer of hydrated matrices HPMC inhibited the transformation of CBZ to its dihydrate form, participated in its crystallization process and caused amorphism of CBZ crystals.

Regarding EA matrix, it was found that EA effect on the conversion rate of CBZ to the dihydrate form and formation of well-developed whiskers depended on the EA concentration. Increasing EA concentration enhanced CBZ dihydrate aggregation. This effect led to the formation of crystals with a high mechanical strength and to the decrease of CBZ dihydrate solubility. Possible mechanisms which explain crystal growth and aggregation as well as alteration of CBZ polymorphic transitions in the gel layer and in aqueous solution were suggested.

The present study was conducted in order to obtain a broader and deeper insight into the mechanism of CBZ release from HPMC and EA matrices. HPMC and EA were selected as hydrophilic carriers in our research because of significant differences of their molecular structures. The different carrier structures might lead to different gel properties which can affect CBZ crystal habit properties and drug release mechanism. We investigated the correlation between hydration properties of the matrices, gel microstructure and mobility, crystalline changes occurring in the gel and drug release kinetics using NMR and EPR techniques. NMR relaxation and EPR spectroscopy are powerful techniques for studying in detail the structure, mobility, and hydration properties of various polymeric systems (3,4). The basic concepts of these techniques were reviewed in our previous paper (5).

MATERIALS AND METHODS

Materials

Trade Egg albumin was obtained from Trima, Israel. Hydroxypropyl methylcellulose (Methocel K4M) was obtained from Colorcon, England. Carbamazepine was obtained from Taro, Israel. 3-carboxy proxyl (PCA), Folin-Ciocalteu's phenol reagent and Dicyclohexyl Carbodiimide (DCC) were purchased from Sigma Chemicals Co, Israel. Sodium dodecyl sulphate (SDS) and sodium hydroxide were purchased from BDH, England. Sodium carbonate was purchased from Frutarom, Israel. Cupric sulphate was purchased from J.T. Baker,

USA. Potassium sodium tartarate and Dimethyl sulfoxide were purchased from Merck, Germany. N-hydroxysuccinimide (NHS) was purchased from Pierce, USA. Deuterium oxide (99.9%) was purchased from Aldrich Chemical Inc., Israel.

Preparation of Tablets

For release experiments, cylindrical tablets were prepared by direct compression of drug-polymer(protein) blends, using a laboratory press (Carver Laboratory Equipment, Carver Inc., USA) fitted with a 10 mm flat-faced punch and die set, and applying 5-ton force. The final tablet weight in all formulations was 0.4g.

Dissolution Studies

The dissolution kinetics of the tablets was monitored using a tablet dissolution tester (model 7ST Caleva, USA). The USP basket method I was used. Rotation speed was 100 rpm (unless otherwise stated) and dissolution medium was 700 ml 1% SDS aqueous solution, maintained at 37°C. CBZ levels were monitored spectrophotometrically (Uvikon 930 Kontron spectrophotometer, Switzerland) at 288 nm. Dissolution studies were performed at least in triplicate for each batch of tablet.

Erosion Studies

The erosion rates of the EA matrices were studied simultaneously with drug release experiments using the Lowry method (6) at 730 nm. The erosion rates of HPMC matrices were determined gravimetrically. At various time intervals the tablets were removed from the baskets and dried for at least 24 h at 37°C until a constant weight was obtained. The percentage of tablet eroded was calculated from the weight loss of the tablets.

EPR Measurements

Preparation of Tablets

For EPR measurements, at 9.4 GHz, the nitroxide, 3-carboxy-proxyl (PCA), was dissolved in acetone, added to the polymer (protein) powder and mixed thoroughly to allow even distribution of the spin label. After the acetone was evaporated at room temperature, CBZ was added to the polymer(protein)-nitroxide mixture and mixed thoroughly in order to obtain homogeneous distribution of the nitroxide in the mixture. The final nitroxide concentration in the mixture was 3–7 mmol/kg. Tablets were prepared, using a laboratory press fitted with an 8 mm flat faced punch and die set, and applying 5-ton force. Tablet weight was 50 mg and the final tablet thickness was 0.8 mm. When PCA conjugated to EA was used as matrix carrier, the EA-PCA conjugate was mixed thoroughly with CBZ and then compressed into tablets.

Preparation of Egg Albumin-3-Carboxy-Proxyl (EA-PCA) Conjugate

A solution of N-hydroxysuccinimide-3-carboxy-proxyl was prepared: 3-carboxy-proxyl; 100 mg, N,N' Dicyclohexyl carbodiimide (DCC); 166.2 mg and N-hydroxysuccinimide (NHS); 92.7 mg were dissolved in 10 ml of dimethyl sulfoxide

(DMSO) and stirred for 24 hours at room temperature. A protein solution containing 20 mg/ml EA was prepared by dissolving EA in 15 ml sodium borate buffer (pH 8.8). 5 ml of the NHS-3-carboxy-proxyl ester was added to the protein solution, mixed well and incubated at room temperature for 4 hr. 8 μ l of 1 M NH_4Cl was added to the protein-3-carboxy-proxyl amide solution. The solution was incubated for 10 min at room temperature and extensively dialyzed against distilled water for at least 24 hours to remove the uncoupled NHS-3-carboxy-proxyl ester (7).

Sample Preparation for EPR Measurements

Tablet Hydration. Tablets, prepared as described previously, were hydrated in 10 ml 1% SDS aqueous solution, at room temperature. At various time intervals the tablets were removed and handled without mechanical damage. The water film at the surface was removed by blotting carefully with an absorbent paper. The tablets were loaded into an EPR teflon device (Physical store, The Hebrew University of Jerusalem, Israel).

Gel Preparation. EA and HPMC solutions and gels in the concentration range 1–16.6% w/w were prepared with 10 μ M PCA in water, at room temperature. The solutions and gels were loaded into capillary tubes or quartz flat-cell, depending on medium viscosity. Gel microviscosity was calculated as described below.

Measurements of EPR Spectra. X-band (9.4 GHz) EPR spectra were recorded using a Joel, JES-RE3X spectrometer with the following settings: field center, 329 mT; scan range, 5.0 or 7.5 mT; scan time, 1 m; time constant, 0.1 sec; microwave power, 1-4 mW (depending on water content in sample); modulation amplitude, 0.1 mT. All measurements were performed at room temperature.

Spectra Analysis

Line-Width and Line-Shape Analysis. Several experimental EPR spectra were a superposition of spectral contributions from mobile (solubilized) and immobile (nonsolubilized) nitroxide molecules. The analysis of the EPR spectra was performed by means of Bruker Winepr software (Version 2.11) in the following way. The immobile spectrum was stimulated in such a way that the outer lines of the simulated and experimental spectra overlapped. The mobile (solubilized) part of the experimental spectrum remained after subtraction of the simulated immobile spectrum. It has been shown that if the radical is placed in a viscous fluid, the line width of each component ($M_I = +1, 0, -1$) has the form (8):

$$T(M) = \alpha + \beta M_1 + \gamma M_I^2 \quad (1)$$

Coefficient α , is a constant term including all line-broadening effects which are the same for all hyperfine components. Coefficients β and γ depend on the anisotropy in g and of the hyperfine splitting, A , and on the mean tumbling rate (set by solvent viscosity), that is the molecular correlation time.

The line-width (α , β , γ parameters) and line-shape (lorentzian/gaussian ratio) simulations of the mobile part of the experimental spectrum were done using Winepr SimFonia program Version 1.25.

Determination of Rotational Correlation Time of Nitroxide in Hydrated Tablets. The immobile spectrum was subtracted from the EPR spectrum as described above. The ro-

tational correlation time (τ_c) of the spin probe in the gel (subtracted spectrum) was calculated from the γ -parameter, using the equation (9):

$$\tau_c = 8\gamma/b^2 \quad (2)$$

where γ is determined from line width simulations (eq 1), $b = 2\pi(A_{zz} - a_0)$ and $a_0 = 1/3(A_{zz} + A_{yy} + A_{xx})$. A , b and γ values are expressed in MHz units.

Microviscosity Calculations. For microviscosity calculations, the following approach was used: PCA was dissolved in water and mixed with glycerol at different ratios. The solutions were loaded into capillary tubes and the EPR spectra of the water-glycerol solutions was recorded using X-band (9.4 GHz) spectrometer as previously described. The rotational correlation time of the PCA in water-glycerol solutions was calculated as described in the previous section. The viscosity of solutions was obtained from Merck Index (10). For determination of microviscosity of the gels and hydrated matrices the $\tau_{c(sec)}$ of the recorded spectra as function of viscosity (cps) was used as calibration curve; $\tau_{c(sec)} = 2.227 \times 10^{-13} + 9.703 \times 10^{-12} \times (\text{viscosity (cps)})$, $r = 0.999$ (13).

Determination of the Mobile/Immobile Compartment in the Tablet. The immobile spectrum was subtracted from the recorded EPR spectrum (mobile+immobile) as described in the line-width and line-shape analysis section. The estimation of mobile compartment was calculated using the equation:

$$\text{mobile compartment (\%)} = \left[\frac{\int \int \text{mobile (subtracted) spectra}}{\int \int \text{mobile + immobile spectra}} \right] * 100 \quad (3)$$

The immobile compartment was calculated by subtracting the percent of the mobile compartment from 100%.

Determination of Rotational Freedom of PCA Conjugated to the Protein. The determination of relative rotational freedom of the nitroxide was based on the following considerations (11,12). The distance between outer wide extremes of EPR spectrum of completely immobilized spin-label equals $2A_{zz}$, where A_{zz} is the maximal principal value of the electron-nuclear hyperfine tensor \hat{A} . (the other two principle values of \hat{A} are designated A_{xx} and A_{yy}). In the common case, when the spin-label is not completely immobilized the distance between outer wide extremes of EPR spectrum is $2\bar{A}_{II}$. This value decreases, as spin-label motion becomes more rapid. If spin-label is fixed rigidly to a protein molecule (for example if it does not contain a spacer as in our case), $2\bar{A}_{II}$ depends only on the rotational correlation of macromolecule (13). To describe the molecular motion of the spin label we used the order parameter S (14).

$$S = \frac{\bar{A}_{II} - \bar{A}_{\perp}}{A_{ZZ} - 1/2(A_{XX} + A_{YY})} \quad (4)$$

Where \bar{A}_{II} and \bar{A}_{\perp} are measured from the experimental spectra and A_{xx} , A_{yy} , A_{zz} are the principal values measured in the absence of molecular motions and in environment of similar polarity. Since,

$$1/3(A_{zz} + A_{xx} + A_{yy}) = 1/3(\bar{A}_{II} + 2\bar{A}_{\perp}) = a_0 \quad (5)$$

where a_0 -isotropic hyperfine constant of the nitroxide radical, then equation 5 can be rewritten as (15):

$$S = \frac{\bar{A}_{II} - a_0}{A_{zz} - a_0} \quad (6)$$

This expression is more useful than eq 4 since a_0 is more easily available from the experiment than A_{xx} and A_{yy} .

The value of $S = 1$ corresponds to an immobile spin-label motion, while $S = 0$ corresponds to an entirely mobile spin-label.

Measurements of Viscosity

Viscosity measurements of EA solutions were performed with Brookfield Model DV-III rheometer at 20°C.

NMR Relaxation Studies

Preparation of Tablets

For NMR relaxation studies, tablets were prepared by direct compression of drug-polymer/protein blends, using a laboratory press fitted with a 3 mm flat-faced punch and die set, and applying 1-ton force. The final tablet weight in all formulations was 30 mg.

Sample Preparation

5-mm standard NMR tubes were filled with double distilled water containing 1% SDS and 11 tablets (arranged as a long cylinder) were inserted at once into the bottom of the tube using a rod. The T_1 and T_2 relaxation times of water as function of time were immediately recorded. The tablets formed a long cylinder inside the NMR tube with a length of approximately 4-cm.

T_1 and T_2 Relaxation Measurements

The T_1 relaxation time of water in the tablets was determined by an inverse recovery sequence (180° - τ - 90° -acquire) (16). Because of the rapid matrix hydration and consequently the rapid change of relaxation times (T_1 , T_2), the minimum time necessary for relaxation measurements was used. Two time delays were used for each measurement ($\tau = 1.0, 2.2$ sec). The results were fitted to the equation; $I = I_0(1 - \exp(-t/T_1))$ and a bracket and binary search routine was used to determine T_1 . The results were consistent with the 32 point T_1 experiment, which showed the same T_1 value to within a few percent; (measured after 2-h hydration).

The T_2 transverse relaxation behavior of water in the tablets was determined using Carr-Purcell-Meiboom-Gill (CPMG) pulse sequence [90_x -(τ - 180_y - τ) $_n$] (16). The n values used were 2 and 16, which were equivalent to a time sequence of 40 and 320 msec. The results were fitted to the equation $I = I_0 \exp(-t/T_2)$. The two-point experiment yielded results consistent with the analysis of a 32-point experiment, which showed the same T_2 value to within a few percent; (measured after 2-h hydration). The T_1 and T_2 relaxation experiments were performed on a Bruker DRX 400 spectrometer. All relaxation measurements were conducted at 25°C.

Self Diffusion Coefficient (SDC) Measurements

Preparation of Gels for SDC Measurements

EA and HPMC solutions and gels in the concentration range 1–66% (EA) and 1–28.7% w/w (HPMC) were prepared

with D₂O. HPMC and EA gels especially at high polymer/protein concentrations were difficult to load into 5-mm NMR tubes because of their high viscosity. Therefore, the gels were first loaded into 4-mm tubes (two-sided hollowed cylinder) having a length of 5 mm, after which the tubes were loaded into 5-mm NMR tubes.

SDC Measurements by NMR

The SDC measurements were performed in D₂O based on the method established by Tanner (17). We used the pulsed field gradient stimulated spin-echo (STE) method (17–19). The pulse sequence consists of three pulses 90°-90°-90° which generates two stimulated field gradient pulses of duration, δ , during the τ periods. The integrated peak intensity I , of the species of interest is given by:

$$I = \frac{I_0}{2} e^{\frac{\tau_1}{T_1} - \frac{2\tau_2}{T_2} - (\gamma G \delta)^2 D \left(\Delta - \frac{\delta}{3} \right)} \quad (7)$$

Where I and I_0 are the echo intensities with and without the field gradient, respectively; τ_1 is the time between the second and third pulses; τ_2 is the time between the first two pulses; T_1 and T_2 are the longitudinal and transverse relaxation times of the species, respectively; γ is the gyromagnetic ratio; G is the magnitude of the field gradient pulses; D is the self diffusion coefficient; δ is the gradient pulse length; and Δ is the time from the start of the first gradient pulse until the start of the second. The SDC, D , of water was extracted utilizing its 4.6-ppm (HDO/H₂O) resonance. Typically, experiments were performed keeping all parameters constant while incrementing G . The SDC was determined from the non-linear regression of the integrated peak intensity I against G^2 .

The NMR experiments were performed on a Bruker DRX 400 spectrometer with BGUII gradient system capable of 56 G/cm. The gradient was calibrated using a cylindrical glass phantom sandwiched between two glass tubes and a hollow glass cylinder sandwiched between glass rods and recording the ¹H or ²H NMR spectrum of the phantom immersed in solvent with the gradient on.

Standard 5-mm NMR tubes were used for all measurements. All measurements of diffusivity were conducted at 25°C. The temperature was determined using a standard methanol NMR thermometer.

RESULTS AND DISCUSSION

CBZ Release Mechanism from the Matrices

CBZ release kinetic from HPMC matrix occurred by the surface erosion mechanism (pseudozero-order release). This was indicated by the similar drug release and matrix erosion rates. In contrast, as discussed in our previous paper, CBZ release from EA matrix was controlled by the bulk erosion mechanism and CBZ crystallization in the gel as the dihydrate form (2).

In order to understand the molecular mechanism of CBZ release from the matrices, gel microstructure was investigated using NMR and EPR techniques.

Investigating of Water Mobility in HPMC and EA Matrices

To investigate water mobility within HPMC and EA matrices, T_1 and T_2 relaxation rates of water were measured

using the NMR technique (Figure 1a,b). The experimental design of our system allowed mainly radial penetration of water into the tablets. Since only minute amounts of water filled the space between the tablet and the NMR tube wall, the T_1 and T_2 relaxation rates were affected mainly by the bound water hydration. The T_1 and T_2 relaxation rates of water increased as a function of time, reflecting the decrease in the tumbling frequency of water due to the increase in the number of hydrogen-bonding interactions to polymer/protein side groups. T_1 water relaxation rates were similar for both formulations indicating that the macroviscosity of the gels was similar. The T_2 relaxation rates were higher in matrices containing HPMC, indicating higher chain hydration of HPMC.

Investigating Gel Mobility

In order to characterize water mobility within the protein and polymer gels, the SDC of water in EA and HPMC was studied for a large concentration range using the NMR technique. It was found that water diffusion was lower in HPMC gels compared with EA gels. Regarding EA, Wang's prediction (20) that the SDC should depend linearly on the volume fraction of the protein applied; $D_w = D_w(0)(1 - \alpha\phi)$ ($r = 0.998$), where ϕ is the volume fraction of the protein and $\alpha = 1.451$ (a value of $\alpha = 1.5$ is applicable to spherical particles). This relationship is one of the several used to describe the so-called "obstruction effect", and predicts a generally similar reduction in diffusion for dilute network systems in which there are

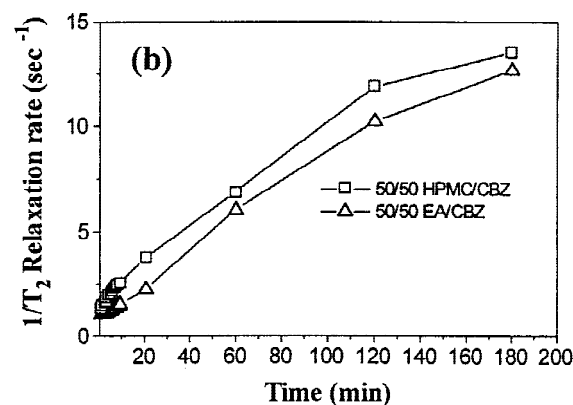
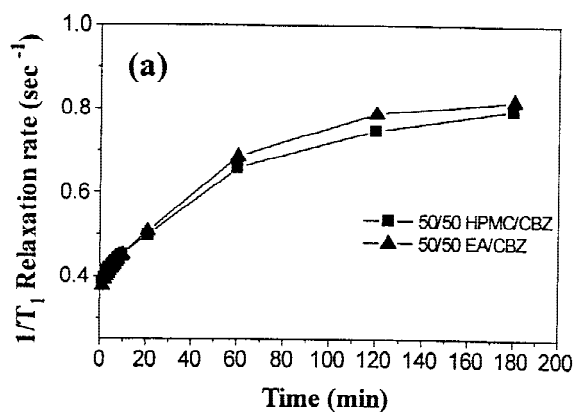


Fig. 1. (a) $1/T_1$; (b) $1/T_2$ relaxation rate of water in matrices containing 50/50 HPMC/CBZ and 50/50 EA/CBZ.

no specific interactions between diffusant and macromolecule (21,22).

Regarding HPMC, water diffusivity, D_w , could be approximately described as an exponential function of the polymer concentration (w/w), C : $D_w = D_w(0) \exp(-KC)$ ($r=0.998$), where $D_w(0)$ is the SDC of water extrapolated to infinite dilution and K is a constant indicative of the retarding effect of the polymer. In HPMC gels $D_w(0) = 21 \times 10^{-6} \text{ cm}^2/\text{s}$ and $K=2.8$. The diffusional behavior of water described by the exponential equation can be related to the Yasuda model (23) which is considered one of the most useful models for describing diffusion of small molecules in moderately swollen gels (24,25). The results suggest formation of an entangled three dimensional network structure in HPMC gels, compared with a diluted network structure for EA, in which the ratio $D_w/D_w(0)$ is approximately independent of the association of the globular EA molecules that form an extended network structure.

Although SDC measurements revealed significantly lower diffusion values of water in HPMC gels, The microviscosity calculations of the corresponding gels, using the EPR technique, revealed similar values for EA and HPMC gels. The microviscosity values were in the range of 2.440 ± 0.063 and 2.472 ± 0.089 cps for EA and HPMC gels respectively (in the concentration range 1–16.6% (w/w) protein/polymer). The results imply that while SDC values are affected by polymer/protein concentrations, the microviscosity values are less sensitive to this effect. This difference can be explained by the fact that the tumbling of water is affected by its interaction with polymer hydroxyl groups an effect that leads to considerable reduction of the SDC values. In contrast, the microviscosity parameter is affected by the tumbling rate of the nitroxide and is related to gel microstructure and the bulk water content.

Correlation Between Gel Microviscosity and Crystalline Properties

Since PCA has M.W. in the same order as CBZ, the calculated microviscosity values reflect the environment to which CBZ is exposed to, in the gels and hydrated matrices. It was suggested in the literature that inhibition of drug crystallization in different polymorphic forms is related to medium viscosity (26,27). We propose that the crystallization of the drug as the dihydrate form (in the molecular level) might be related to medium microviscosity (rather than viscosity). Increase of solution microviscosity, may induce a suppressive effect on the nuclei formation and solvent mediated growth of the nuclei formed during the crystallization process. Based on the results of our previous investigation combined with the results of the present study it can be concluded that although EA and HPMC gels are characterized by low microviscosity values (close to water), HPMC inhibits the crystallization of CBZ as the dihydrate form compared with partial inhibition effect of EA. These findings strengthen our suggestion presented in our previous research regarding specific interaction between HPMC and CBZ, which inhibits CBZ conversion to the dihydrate form (1,2). This interaction was proposed to occur through hydrogen binding; the hydroxyl groups on the polymer are attached to CBZ at the sites of water binding and thus inhibit its transformation to the dihydrate form.

In order to get a deeper insight into matrix properties, we

investigated the gel structure and hydration properties of the matrices using the EPR technique. EPR studies performed at a frequency of 9–10 GHz (X-band) are limited to aqueous sample thickness less than 1 mm due to high non-resonant dielectric losses caused by water content in the sample. Therefore, our measurements were limited to thin tablets (< 1mm) and to the initial hydration of the matrices, where matrix swelling was minimal. We assume that the changes in the recorded EPR spectra of the hydrated tablets can be used to characterize the gelation process occurring in the outer surface of the matrices.

Figure 2a,b presents the EPR spectra (first derivative) of hydrated matrices containing 50/50 HPMC/CBZ and 50/50 EA/CBZ at various time intervals. Figure 3a,b presents the corresponding integrated spectra of the formulations studied. The integrated spectrum is more useful than the first derivative spectra for estimating the mobile/immobile compartment. The contribution of the mobile species is more pronounced in the first derivative spectrum due to the narrow line-width, however, in the integrated spectra the contribution of the immobile component can be more clearly seen. The EPR spectra of the dry tablets indicate a high immobilization of the nitroxide, typical for solid samples with randomly oriented nitroxides. Exposure to 1% SDS aqueous solution led to changes in the spectral shape. The EPR spectra consisted of a superposition of immobilized and highly mobile PCA, indicating the formation of a low viscous compartment in the tablet. The integrated EPR spectra of hydrated HPMC/CBZ and EA/CBZ indicate a higher immobile compartment in matrices containing HPMC.

Table 1 summarizes the mobile compartment of PCA in the hydrated tablets, the rotational correlation time of PCA and the corresponding microviscosity values of the hydrated tablets. The rotational correlation time and microviscosity values were found to be lower in formulation containing 50%

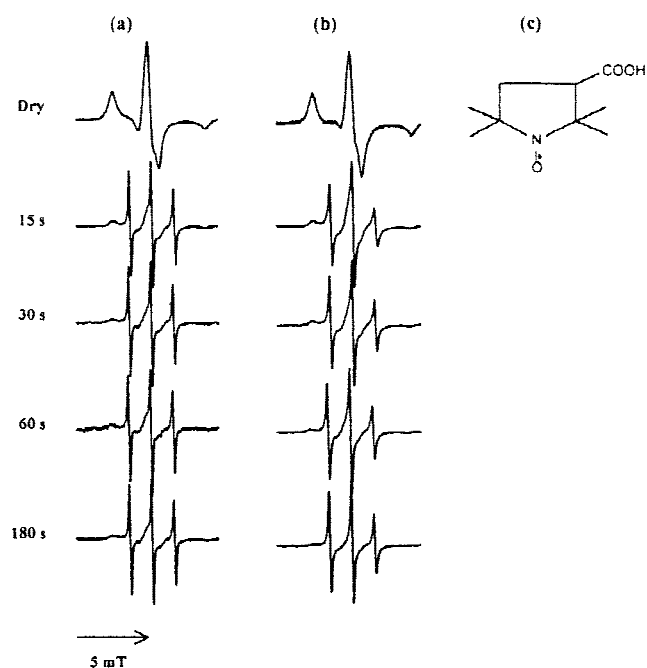


Fig. 2. EPR spectra of hydrated matrices containing (a) 50/50 HPMC/CBZ; (b) 50/50 EA/CBZ. (c) PCA structure. (Unbound PCA).

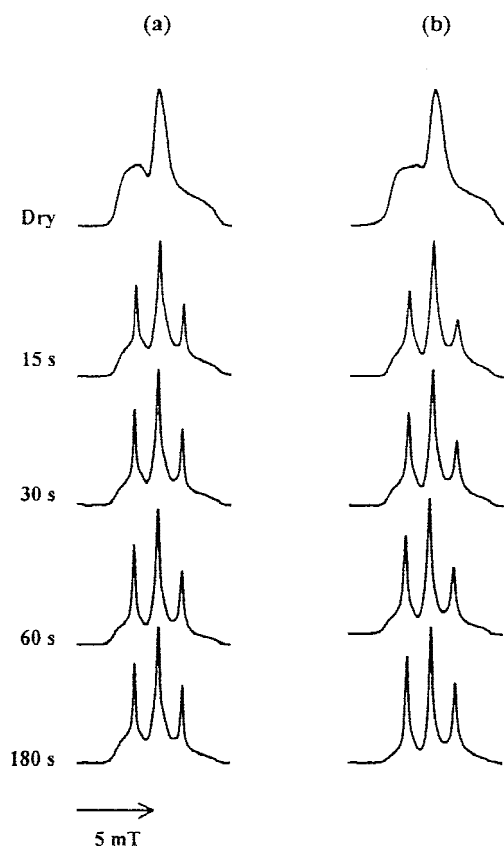


Fig. 3. Integrated EPR spectra of hydrated matrices containing (a) 50/50 HPMC/CBZ; (b) 50/50 EA/CBZ. (Unbound PCA).

HPMC compared with 50% EA. The lower microviscosity is explained by the higher water binding and absorption of HPMC matrices compared with EA. It should be emphasized that our measurements were limited to initial hydration times where matrix erosion was insignificant. It is expected that at longer times, the bulk erosion of EA matrices would significantly increase the amount of bulk water in the matrix, which would lead to lower microviscosity values. Both HPMC and EA microviscosity values are expected to approach the microviscosity of water at longer hydration times. Table 2 summarizes the line-width (α , β , γ parameters) and line-shape (G) simulations of the respective EPR spectra. In the HPMC formulation the α , β , γ parameters approach zero more closely. The contribution of the gaussian line-shape was

slightly higher in the HPMC formulation compared to EA (after 1 and 3 min).

Correlation Between Drug Release Kinetics, Matrix Erosion, Matrix Structure and Crystalline Properties

HPMC and EA matrices showed different erosion mechanisms, which influenced the respective CBZ release kinetics from the matrices. CBZ was released from HPMC matrix by surface erosion mechanism compared to EA matrix in which CBZ release was influenced by matrix bulk erosion mechanism and CBZ crystallization as the dihydrate form.

The different modes of matrix erosion stem from the different structures of EA and HPMC molecules. While HPMC should undergo a process of disentanglement in order to be released from the matrix, a process which occurs at the outer surface of the matrix (gel matrix-diffusion layer interface), EA which is a globular protein does not undergo a process of disentanglement and once hydrated it is released from the matrix by diffusion. Therefore, the process of EA bulk erosion occurs throughout the whole portion of the matrix and is not confined to the diffusion layer interface.

Support for the different erosion modes of the matrices is provided by the viscosity values of these molecules. It is known that molecules undergoing chain entanglement are characterized by strong viscosity dependence on concentration. The viscosity of 2% (w/v) aqueous HPMC solution is 4000 cps compared with a value of 3 cps for EA.

Using NMR T_2 relaxation studies it was shown that HPMC matrices are characterized by higher chain hydration compared to EA matrices indicating higher water binding sites for HPMC matrices. Since HPMC is an entangled polymer, chain hydration leads to breakage of polymer-polymer contacts, increase of polymer hydrodynamic volume and therefore to higher matrix swelling compared to EA.

The water SDC in HPMC gels could be described by the Yasuda model compared to EA gels in which Wang's model applied. Measurements of SDC in the gels supported the formation of an entangled three-dimensional gel structure in HPMC compared to diluted network structure for EA. The formation of diluted network structure for EA with low protein-protein interactions allows the protein diffusion from the matrix interior. These properties of HPMC and EA gels led to matrix surface erosion and bulk erosion mechanisms respectively.

Although viscosity and SDC values were affected by polymer (or protein) concentrations and the type of the dissolved macromolecule (HPMC or EA), the microviscosity

Table 1. Mobile Compartment (%), Rotational Correlation Time of PCA and Microviscosity Values of 50/50 HPMC/CBZ and 30/70, 50/50, 70/30 EA/CBZ Hydrated Matrices

Time (sec)	Mobile compartment (%)				Rotational correlation time ($\tau_c \times 10^{10}$, sec)				Microviscosity (cps)			
	HPMC/CBZ		EA/CBZ		HPMC/CBZ		EA/CBZ		HPMC/CBZ		EA/CBZ	
	50/50	30/70	50/50	70/30	50/50	30/70	50/50	70/30	50/50	30/70	50/50	70/30
15	31.48	64.16	47.81	28.73	0.470	1.04	2.30	2.61	4.82	10.7	23.6	26.9
30	38.33	69.26	55.04	32.78	0.440	0.913	1.44	2.09	4.55	9.38	14.7	21.5
60	45.55	76.12	64.54	51.50	0.404	0.626	1.04	1.44	4.14	6.43	10.7	14.8
180	61.03	84.26	71.04	53.09	0.313	0.470	0.913	1.30	3.20	4.81	9.38	13.4

Table 2. Line-Width and Line-Shape Simulations of 30/70, 50/50 and 70/30 EA/CBZ EPR Spectra

Time (sec)	50/50 HPMC/CBZ				30/70 EA/CBZ				50/50 EA/CBZ				70/30 EA/CBZ			
	α	β	γ	G*	α	β	γ	G	α	β	γ	G	α	β	γ	G
15	1.21	-0.12	0.18	100	1.64	-0.16	0.40	100	1.80	-0.37	0.88	100	1.90	-0.50	1.00	100
30	1.10	-0.11	0.17	100	1.55	-0.13	0.35	95	1.50	-0.28	0.55	100	1.72	-0.40	0.80	100
60	1.00	-0.10	0.155	100	1.50	-0.11	0.24	80	1.50	-0.25	0.40	90	1.50	-0.35	0.55	90
180	1.00	-0.09	0.12	100	1.30	-0.09	0.18	80	1.35	-0.15	0.35	90	1.50	-0.28	0.50	90

* G: gaussian contribution (%).

The lorentzian (L) contribution is calculated by subtracting the gaussian contribution from 100%.

The L/G ratio is calculated from the L and G contribution.

values measured by EPR were less sensitive to this effect. The microviscosity values measured by EPR reflect the environment to which the drug is exposed to in the gels and hydrated matrices. The microviscosity values were similar for EA and HPMC in the concentration range 1–16% (w/w). Since in our previous study we showed that in this concentration range HPMC completely inhibited CBZ transformation to its dihydrate form compared to partial inhibition (depending on EA concentration) for EA, it can be concluded that the retardation of CBZ transformation to its dihydrate form is not related to gel microviscosity.

In hydrated matrices the results showed that HPMC and EA are characterized by microviscosity values close to water with higher initial microviscosity for EA which can be explained by its initial lower water binding capacity.

In a previous study we showed that HPMC inhibits CBZ transformation to the dihydrate form and induces amorphism of CBZ crystals with the formation of spherulite structure of CBZ in hydrated matrices. It was suggested that the interaction between HPMC and CBZ occurs through hydrogen binding. By contrast EA matrices behaved differently and CBZ was transformed to its dihydrate form as a function of hydration time and matrix erosion. The finding that the microviscosity values of the hydrated HPMC matrices were lower than EA and approached the value of water suggests that the inhibition of HPMC transformation to its dihydrate form is not related to the environment microviscosity. This supports our hypothesis concerning a specific interaction between HPMC and CBZ.

The contribution of the gaussian line-shape was found to be slightly higher for HPMC matrices compared to EA (after 1 and 3 min), implying that the structure formed was more heterogeneous (containing a higher number of components with distinct microviscosities) in formulation containing HPMC. This is attributed to the crystallization of CBZ in the gel as the amorphous form. Support for this conclusion is provided by the fact that the same formulation containing naproxen, which does not undergo such crystalline changes, was characterized by significantly lower gaussian contribution (60%) compared with 100% for CBZ formulation.

The lower mobile compartment in matrices containing HPMC may be attributed to the higher water binding capacity of HPMC chains, which retards water penetration into the dry core. By contrast, because of the lower content of hydrophilic water-binding groups on protein surface compared with HPMC, the water molecules penetrating the matrix are interacting to a lesser degree with protein and therefore the penetration rate into the dry matrix core is higher.

Correlation Between CBZ Release Kinetics from EA Matrices and Matrix Microstructure: The Effect of EA Concentration on Matrix Properties

The Effect of EA Concentration on Matrix Microstructure

In our previous paper (2) we showed that the influence of EA on CBZ release is anomalous. Decreasing EA concentrations in the matrix decreased drug release. We proposed that this effect is related to the increased crystallization of CBZ as the dihydrate form in matrices containing lower concentrations of EA. In order to obtain a deeper understanding of the mechanism involved in CBZ release from EA matrix we measured the T_1 and T_2 relaxation rates, microviscosity and mobile/immobile compartment of these formulations using NMR and EPR spectroscopy.

NMR Relaxation Studies

Figure 4a,b presents the NMR T_1 and T_2 relaxation rates of water in the matrices. T_2 relaxation rates were higher for formulation containing 70/30 EA/CBZ compared with formulations containing lower concentrations of EA. This behavior of the EA/CBZ matrix reflects the increase of water binding capacity of EA with the increase of EA concentrations. It is known that crystalline water is characterized by higher T_2 relaxation rates compared with water bound to protein/polymer (28). The initial higher water relaxation rate in matrices containing 30/70 EA/CBZ compared with 50/50 EA/CBZ may reflect the higher conversion rate of CBZ to its dihydrate form in formulations containing lower concentrations of EA, as discussed in our previous research (2). Figure 4a revealed that T_1 relaxation rates of water increased with increasing EA concentrations in the matrix. Since the T_1 relaxation rate is related to the water mobility within the gel, the results imply higher gel macroviscosity in matrices containing higher concentrations of EA.

EPR Studies

In order to characterize the gel microstructure and protein chain relaxation and to correlate between these effects, drug release mechanism and matrix erosion, we analyzed the EPR spectral parameters of matrices containing PCA in two states: unbound and bound to protein chains.

EPR Spectra Analysis of Unbound PCA

Figure 5a,b,c presents the EPR first derivative and integrated spectra of formulations containing different EA/CBZ ratios. Table 1 summarizes the calculated mobile compartment, rotational correlation time of PCA in the hydrated tablets and the corresponding microviscosity values. Increasing EA concentration retarded water penetration into the matrix

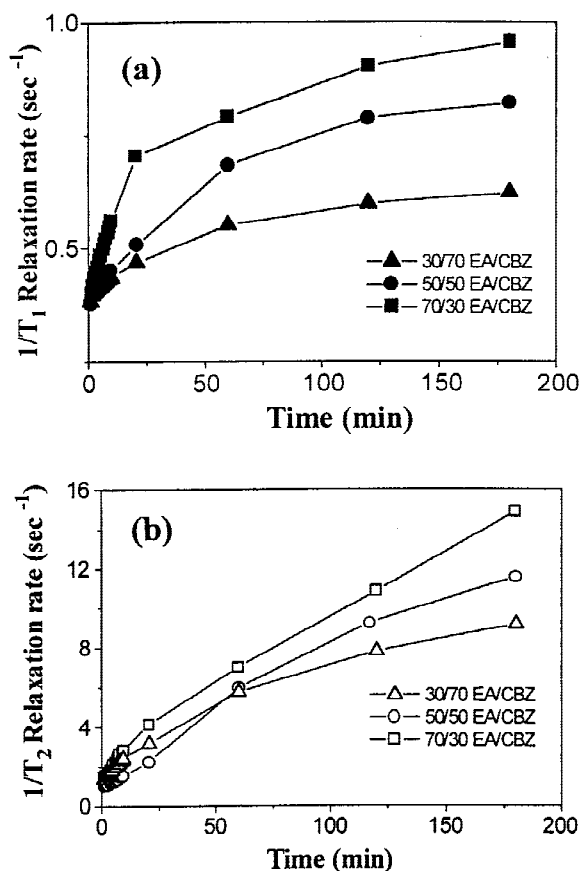


Fig. 4. (a) $1/T_1$; (b) $1/T_2$ relaxation rates of water in matrices containing 30/70 EA/CBZ, 50/50 EA/CBZ and 70/30 EA/CBZ.

and correspondingly decreased the mobile compartment (solubilized PCA). Increasing EA concentration in the matrix increased the rotational correlation time of PCA and correspondingly the microviscosity values increased. Matrices containing 30/70 EA/CBZ were characterized by the lowest rotational correlation time and microviscosity values.

These results are in correlation with the T_1 , T_2 relaxation data and provide further support to our previous findings (2). Increasing EA concentration in the matrix increased gel microviscosity and therefore retarded the conversion of CBZ to its dihydrate form. Based on these results it can be concluded that matrices containing the lowest EA content (30/70 EA/CBZ) are characterized by the lowest gel microviscosity, highest conversion of CBZ to its dihydrate form, an effect which led to slower CBZ release from the matrix.

Table 2 summarizes the line-width (α , β , γ parameters) and line-shape (G) simulations of the respective EPR spectra. Line-width simulations revealed that the α , β , γ parameters approach zero more closely in formulations containing lower concentrations of EA, further supporting the lower microviscosity in matrices containing 30/70 EA/CBZ compared with 50/50 and 70/30 EA/CBZ matrices. Line-shape simulation revealed that increasing EA concentrations in the matrix increased the contribution of gaussian line-shape. This implies that the structure formed was more heterogeneous (containing a higher number of components) in formulations containing higher concentrations of EA. Inhomogeneous line broadening (gaussian line-shape) may occur when the number of

hyperfine components from nearby nuclei is large, hence one detects an envelope of a multitude of lines. In our system, the mechanism contributing to inhomogeneous line broadening may result from the super-hyperfine interaction between the methyl protons and the nitrogen atom in PCA molecule (Figure 2c). The super-hyperfine interaction depends on the mobility of the molecule (increasing medium viscosity will decrease the tumbling rate of the nitroxide and therefore the contribution of gaussian line-shape will increase) and the relative arrangement of the methyl groups to the NO-group. In the 30/70 EA/CBZ formulation the lower contribution of gaussian line-shape is influenced by the lower gel microviscosity compared with the formulations containing higher concentrations of EA.

EPR Spectra Analysis of Bound PCA

In order to examine the effect of EA concentration in the matrix on protein chain relaxation, PCA was bound to EA and PCA-EA conjugate was used as a matrix carrier. The EPR first derivative and integrated spectra of formulations containing 30/70 PCA-EA/CBZ, 50/50 PCA-EA/CBZ and 70/30 PCA-EA/CBZ is presented in Figure 6a-c. It can be concluded that the mobile compartment of PCA in the unbound state (Figure 5) was higher compared with PCA in the bound state (Figure 6). This difference is attributed to the fact that the PCA in the unbound state is affected by the bulk water which penetrated the matrix compared with PCA in the con-

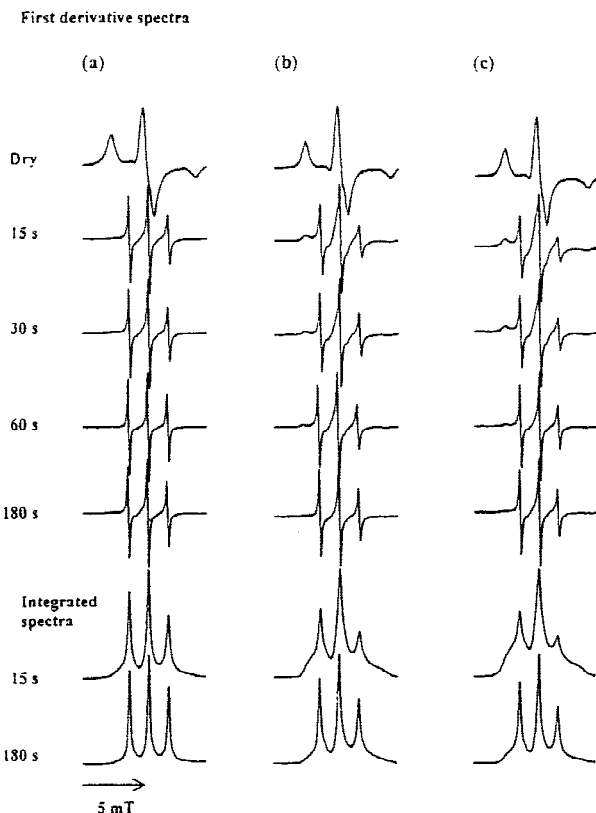


Fig. 5. EPR first derivative and integrated spectra of hydrated matrices containing (a) 30/70 EA/CBZ; (b) 50/50 EA/CBZ; and (c) 70/30 EA/CBZ. (Unbound PCA).

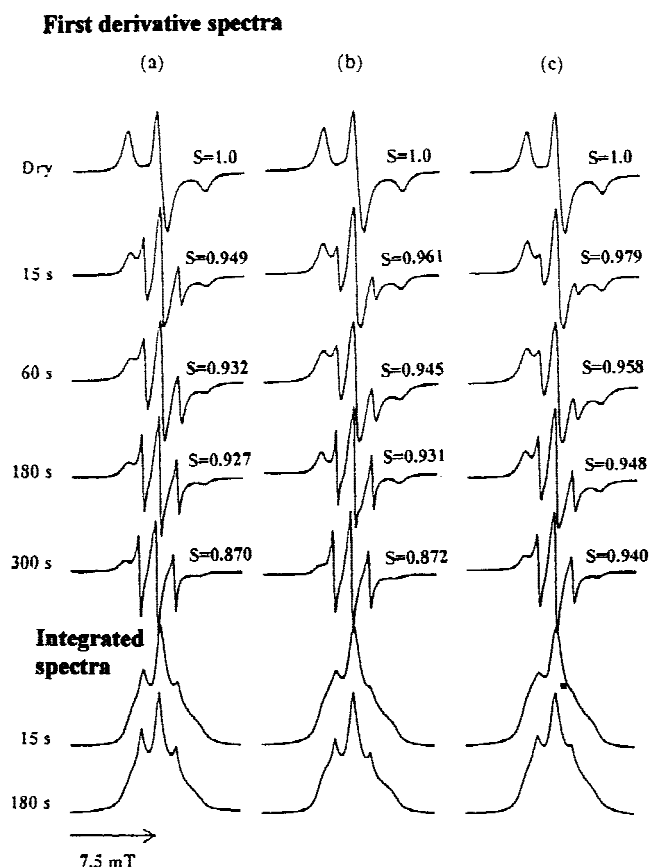


Fig. 6. EPR first derivative and integrated spectra of hydrated matrices containing (a) 30/70 PCA-EA/CBZ; (b) 50/50 PCA-EA/CBZ; and (c) 70/30 PCA-EA/CBZ. (Bound PCA).

jugated state which is affected by the hydration and relaxation of protein chains, a slower process. When comparing the EPR spectra (first derivative and integrated spectra) of the three formulations containing PCA-EA, it is revealed that the mobile compartment, indicating chain hydration and mobility, is lower in formulations containing higher concentrations of EA. These results are in correlation with the erosion properties of the matrices, which showed a higher fraction of immobilized EA that remained in the matrix in formulation containing 70/30 EA/CBZ compared with 50/50 EA/CBZ and 30/70 EA/CBZ. EA release from matrices containing 70/30 EA/CBZ was lower compared with 50/50 and 30/70 EA/CBZ (2). The results suggest that increasing EA concentrations in the matrix increased protein-protein interaction and gel microviscosity. Consequently, the protein chain mobility and EA release from the matrix decreased.

The S -parameter values calculated according to equation 6 are presented in Figure 6. The results imply that the S -parameter is lower for 30/70 PCA-EA/CBZ matrices compared with formulations containing higher contents of EA. A lower S -parameter value indicates higher chain mobility further supporting our conclusion that formulations containing lower contents of EA are characterized by lower degree of protein aggregation and higher chain mobility.

CONCLUSIONS

The present study was conducted in order to investigate the correlation between the hydration properties of HPMC

and EA matrices, gel microstructure and mobility, crystalline changes occurring in the gel and CBZ release kinetics from the matrices. The influence of HPMC and EA erosion modes on CBZ release kinetic was interpreted in terms of gel microstructures.

Investigation of CBZ release from the matrices revealed that drug release from HPMC matrix was higher and occurred by the surface erosion mechanism (pseudozero-order release) compared to the EA matrix in which matrix erosion occurred by bulk erosion mechanism. The results suggested formation of an entangled three-dimensional network structure in HPMC gels, compared with a dilute network structure for EA. Since EA is a globular protein it does not undergo a process of entanglement in solution and once hydrated it is released from the matrix by diffusion. The EPR and NMR results imply that although there is sufficient mobility in HPMC hydrated matrices, CBZ is not transformed to its dihydrate form in this formulation. This finding supports our hypothesis concerning the mechanism involved in the inhibition of CBZ transformation to its dihydrate form in the presence of HPMC, which occurs through specific interaction with hydroxyl groups of the polymer. The microviscosity and mobile/immobile compartment values in hydrated matrices containing different EA/CBZ ratios were in correlation with the crystallization properties of CBZ in the gels and its release kinetics from the matrices. The mobility values (S -parameter) of PCA conjugated to EA (in PCA-EA/CBZ matrices) were in correlation with EA aggregation and erosion properties of EA/CBZ matrices.

REFERENCES

1. I. Katzhendler, R. Azoury and M. Friedman. Crystalline properties of carbamazepine in sustained release hydrophilic matrix tablets based on hydroxypropyl methylcellulose. *J. Control. Rel.* **54**: 69–85 (1998).
2. I. Katzhendler, R. Azoury and M. Friedman. The effect of egg albumin on the crystalline properties of carbamazepine in sustained release hydrophilic matrix tablets and in aqueous solutions. *J. Control. Rel.* **65**:331–343 (2000).
3. R. Mathur-De Vre. The NMR studies of water in biological systems. *Prog. Biophys. Molec. Biol.* **35**:103–134 (1979).
4. K. Mäder, H. M. Schwartz, R. Stösser and H. H. Borchert. The application of EPR spectroscopy in the field of pharmacy. *Pharmazie* **49**:97–101 (1994).
5. I. Katzhendler, K. Mäder and M. Friedman. Correlation between drug release kinetics from proteineous matrix and matrix structure: EPR and NMR Study. *J. Pharm. Sci.* **89**:365–381 (2000).
6. E. Harlow and D. Lane. *Antibodies A Laboratory Manual*, Cold Spring Harbor Laboratory, 1988, p. 675.
7. E. Harlow and D. Lane. *Antibodies A Laboratory Manual*, Cold Spring Harbor Laboratory, 1988, p. 341.
8. J. E. Wertz and J. R. Bolton. *Electron spin resonance: Elementary theory and practical applications*, McGraw Hill Inc., New York, 1972.
9. P. L. Nordio. General magnetic resonance theory. In: L. J. Berliner (ed.), *Spin Labeling: Theory and Applications*, Academic Press, New York, 1976 pp. 34.
10. M. Windholz, S. Budavari, R. Blumetti, and E. Otterbein. *The Merck Index*, Merck&Co, Inc., New Jersey, 1983 pp. 4347.
11. I. V. Dudich, V. P. Timofeev, M. V. Volkenstein, and A. Y. Misharin. Macromolecule rotational correlation time measurements by ESR method for covalently bound spin-label. *Mol. Biol. (USSR)* **9**:531–538 (1977).
12. V. P. Timofeev, I. V. Dudich, Y. K. Sykulev, and R. S. Nezhin. Rotational correlation times of IgG and its fragments spin-labeled at carbohydrate of protein moieties. Spatially fixed position of the Fc carbohydrate. *FEBS Lett* **89**:191–195 (1978).
13. E. J. Shimshik and H. M. McConell. Rotational correlation time

- of spin-labeled α -chemotripsin. *Biochem. Biophys. Res. Commun.* **46**:321–326 (1972).
14. O. H. Griffith and P. C. Jost. Lipid spin labels in biological membranes. In: L. J. Berliner (ed.), *Spin Labeling: Theory and Applications*, Academic Press, New York, 1976 pp. 454–523.
 15. V. P. Timofeev, I. V. Dudich, and M. V. Volkenstein. Comparative study of dynamic structure of pig and chicken aspartate aminotransferases by measuring the rotational correlation time. *Biophys. Struct. Mech.* **7**:41–49 (1980).
 16. A. E. Derome. Modern NMR techniques for chemistry research. In: J. E. Baldwin (ed.), *Organic chemistry series*; Vol. 6, Pergamon Press, Oxford, 1987 pp. 85–96.
 17. J. E. Tanner. Use of the stimulated echo in NMR diffusion studies. *J. Chem. Phys.* **52**:2523–2526 (1970).
 18. P. Stilbs. Fourier transform pulsed-gradient spin-echo studies of molecular diffusion. *Prog. NMR Spectrosc.* **19**:1–45 (1987).
 19. R. M. Cotts, M. J. R. Hoch, T. Sun, and J. T. Markert. Pulsed field gradient stimulated echo methods for improved NMR diffusion measurements in heterogeneous systems. *J. Magn. Reson.* **83**:252–266 (1989).
 20. J. H. Wang. Theory of the self diffusion of water in protein solutions. A new method for studying the hydration and shape of protein molecules. *J. Am. Chem. Soc.* **76**:4763–4765 (1954).
 21. W. Brown and P. Stilbs. Self-diffusion measurements on bovine serum albumin solutions and gels using a pulsed-gradient spin-echo NMR technique. *Chemica Scripta* **19**:161–163 (1982).
 22. W. Brown and R. M. Johnsen. Diffusion in polyacrylamide gels. *Polymer* **22**:185–189 (1981).
 23. P. Gao and P. Fagerness. Diffusion in HPMC gels. I. Determination of drug and water diffusivity by pulsed-field-gradient spin-echo NMR. *Pharm. Res.* **12**:955–964 (1995).
 24. H. Yasuda and C. E. Lamaze. Permselectivity of solutes in homogeneous water-swollen polymer membranes. *J. Macromol. Sci. Phys.* **B5**:111–134 (1971).
 25. H. Yasuda, C. E. Lamaze, and A. Peterlin. Diffusive and hydraulic permeabilities of water in water-swollen polymer membranes. *J. Poly. Sci. Part A2* **9**:1117–1131 (1971).
 26. E. Shefter and T. Higuchi. Dissolution behavior of crystalline solvated and nonsolvated forms of some pharmaceuticals. *J. Pharm. Sci.* **52**:781–791 (1963).
 27. A. R. Ebian, M. A. Moustafa, A. Said, A. Khalil, and M. M. Motawi. Succinylsulfathiazole crystal forms II: Effects of additives on kinetics of interconversion. *J. Pharm. Sci.* **64**:1481–1484 (1975).
 28. G. D. Fullerton, J. L. Potter, and N. C. Dornbluth. NMR relaxation of protons in tissues and other macromolecular water solution. *Magn. Res. Imag.* **1**:209–228 (1982).